

1-1-2003

Preparation and flammability properties of polyethylene-clay nanocomposites

Jinguo Zhang
Marquette University

Charles A. Wilkie
Marquette University, charles.wilkie@marquette.edu

Marquette University

e-Publications@Marquette

Chemistry Faculty Research and Publications/College of Arts and Sciences

This paper is NOT THE PUBLISHED VERSION; but the author's final, peer-reviewed manuscript.

The published version may be accessed by following the link in the citation below.

Polymer Degradation and Stability, Vol. 80, No. 1 (2003) : 163-169. [DOI](#). This article is © Elsevier and permission has been granted for this version to appear in [e-Publications@Marquette](#). Elsevier does not grant permission for this article to be further copied/distributed or hosted elsewhere without the express permission from Elsevier.

Preparation and Flammability Properties of Polyethylene–Clay Nanocomposites

Jinguo Zhang

Department of Chemistry, Marquette University, Milwaukee, WI

Charles A. Wilkie

Department of Chemistry, Marquette University, Milwaukee, WI

Abstract

Polyethylene (PE)–clay nanocomposites have been prepared using melt blending in a Brabender mixer. X-ray diffraction and transmission electron microscopy were used to characterize the nano-structure of these composites while the thermal stability was evaluated from thermogravimetric analysis and the flammability parameters using cone calorimetry. It is found that the PE–clay nanocomposites have a mixed immiscible-intercalated structure and there is better intercalation when maleic anhydride is combined with the polymer and clay to be melt blended. The reduction in peak heat release rate is 30–40%.

Keywords

Nanocomposites; Polyethylene; Cone calorimetry

1. Introduction

Significant improvements in the physical properties of polymers, including mechanical, thermal and gas barrier properties, have been realized through the production of polymer–clay nanocomposites, which contain only a small amount of clay. Nanocomposites may be prepared either by polymerization of a monomer in the presence of the clay or by blending with the clay. In either case, the sodium cation which occupies the gallery space in the clay must be ion-exchanged with an ‘onium’ salt which contains at least one long organic chain to render the gallery space sufficiently organophilic to permit the entry of the polymer into this gallery space. The formation of a nanocomposite requires that the clay be well dispersed throughout the polymer. When the clay is not well dispersed, the material is referred to as immiscible and the clay is acting as a filler. In the case of a well-dispersed system, if the registry between the clay layers is maintained, the system is described as intercalated, if this registry is lost, the system is called exfoliated or delaminated.

There have been several reports on polyolefin–clay nanocomposites,^{1,2,3,4} but only a few on polyethylene (PE)–clay nanocomposite^{5,6,7} and no work was reported on the flammability of PE nanocomposites. Due to its non-polar backbone, it is a challenge to make PE nanocomposites. Gaylord⁵ has combined very high levels of clay with PE in the presence of maleic anhydride (MA) and has no doubt obtained an immiscible material. Kuchta et al.⁶ have combined PE with an organically-modified clay in a twin-screw extruder and claim the formation of a nanocomposite. Wang et al.⁷ have shown that a nanocomposite may be formed using PE-g-MA when the organically-modified clay contains at least a C-18 chain but the material is at least partially immiscible when the carbon chain is shorter. They claim the formation of exfoliated materials when MA is present and intercalated nanocomposites in the absence of MA.

In this paper melt blending is used to prepare nanocomposites of polyethylene by mixing with clay in the absence or the presence of MA. The materials have been characterized by X-ray diffraction, XRD, thermogravimetric analysis, TGA, transmission electron microscopy, TEM, and cone calorimetry.

2. Experimental

2.1. Materials

Low-density Polyethylene (LDPE) was acquired from Aldrich Chemical Company; it was dried for 2h at 80 °C in an oven then stored over P₂O₅. Maleic anhydride (MA) was also from Aldrich and was used as received. The sodium clay and the organically-modified clays Cloisite 6A, 20A, 25A, 30B were kindly provided by Southern Clay products, Inc. Two additional clays, Si18 and VB16, were prepared following our published literature procedure.⁸ The description of the organic modifiers, the names by which they are known and the d-spacing are shown in Table 1.

Table 1. Structure of ammonium salt and d-space of its clay

| Organically-modified clay | 2 θ | d-Spacing (nm) | Organic modifier |
|---------------------------|------------|----------------|--|
| 6A | 2.58 | 3.4 | Dimethyl dihydrogenated tallow ammonium |
| 20A | 3.64 | 2.4 | Same as above |
| 25A | 4.74 | 1.8 | Dimethyl hydrogenated-tallow (2-ethylhexyl) ammonium |

| | | | |
|------|------|-----|---|
| 30B | 4.70 | 1.9 | Methyl tallow bis(2-hydroxyethyl) ammonium |
| VB16 | 4.36 | 2.0 | Dimethyl- <i>n</i> -hexadecyl-(4-vinylbenzyl) ammonium |
| Si18 | 3.94 | 2.2 | [3-(Trimethoxysilyl) propyl] octadecyldimethyl ammonium |

The difference between 6a and 20A is the concentration of ammonium salt, for 6a is 140 meq/100 g; for 20A is 95 meq/100 g.

2.2. Preparation of PE–clay nanocomposites

The organically-modified clays used in this study may be divided into two sets; those which contain no functionality, e.g. 6A, 20A, and 25A, and those which do contain a functionality, 30B, VB16 and Si18. The clay content was fixed at 3% (mass fraction) for all systems.

2.2.1. PE/clay nanocomposites

LDPE with 3% organically-modified clay, such as Cloisite 6A, 20A or 25A, were premixed in a beaker, then melt blended in a Brabender Plasticorder with a chamber of 50 cm³ at 170 °C. The screw speed was at a low speed, 30 rpm, for the first 5 min, then increased to 60 rpm for 25 min to get a well-mixed system. Upon completion of the blending, the molten composite was removed from the chamber and allowed to cool to room temperature.

2.2.2. PE/MA/clay nanocomposites

LDPE and 3% MA were mixed in a beaker, then added into the Brabender chamber and mixed for 5 min at 170 °C at low speed (30 rpm). Then 3% organically-modified clay, such as VB16, Si18 or Cloisite 30B, was added in small portions. After all of the clay was added, the screw speed was increased to 60 rpm for 25 min. Upon completion of the blending, the molten composite was removed and allowed to cool to room temperature.

2.3. Instrumentation

X-Ray Diffraction (XRD) patterns were obtained using a Rigaku Geiger Flex, 2-circle powder diffractometer equipped with Cu- K_{α} generator ($\lambda=1.5404 \text{ \AA}$). Generator tension is 50 KV and generator current is 20 mA. All the samples were compress molded at 170–180 °C to 20 mm×15 mm×1 mm plaques for XRD measurements. Bright field transmission electron microscopy (TEM) image was obtained at 120 kV, at low-dose conditions, with a Phillips 400T electron microscopy. The sample was ultramicrotomed with a diamond knife on a Leica Ultracur UCT microtome at room temperature to give 70-nm-thick section. The section was transferred from water to carbon-coated Cu grids of 200 mesh. The contrast between the layered silicate and the polymer phase was sufficient for imaging, so no heavy metal staining of sections prior to imaging was required. Thermogravimetric analysis (TGA) was carried out on a Cahn TG131 unit under nitrogen at a scan rate of 10 °C per minute from room temperature to 600 °C. Temperatures are reproducible to ± 3 °C while the fraction of non-volatile is repeatable to $\pm 3\%$. Cone calorimetry was performed on an Atlas CONE-2 according to ASTM E 1354-92 at an incident flux of 35 kW/m² using a cone shaped heater. Exhaust flow was set at 24 l/s and the spark was continuous until the sample ignited. Cone samples were prepared by compression molding the sample (about 25 g) into square plaques. Typical results from Cone calorimetry are reproducible to within about $\pm 10\%$. These uncertainties are based on many runs in which thousands of samples have been combusted.⁹

3. Results and discussion

3.1. Clay structures used in this study

There are two classes of clay that have been used in this study, those which do not contain functionalities and those which are functionalized. The unfunctionalized clays should be incapable to react with the polymer or with MA. The three functionalized clays, 30B, Si18 and VB16 all have different functional groups which may show quite different reactivities. In the case of the clay 30B the functionalities are hydroxyl groups which could react with the maleic anhydride units grafted onto the clay; reaction with PE itself is unlikely. The clay Si18 contains a silicon–oxygen bond which may also react with the maleic anhydride units. The functional group in VB16 is a double bond and this is unlikely to react with either PE or MA.

3.2. Characterization of Nanocomposites by XRD

Polymer–clay nanocomposites are formed by the insertion of polymer chains between the clay layers. As the polymer inserts, it must increase the gallery space and force the clay layers to separate, thus XRD is a suitable means to evaluate this process. The XRD results for the various clays are tabulated in Table 2 and are also presented graphically in Fig. 1, Fig. 2. One sees that there is only a small change in the d-spacing for those systems which were melt-blended without MA and a more substantial difference for those with MA. The clays that show an effect in the presence of MA, VB16, Si18, and 30B, have also been used in the absence of MA and the d-spacing does not change without MA. The XRD of the VB16 system needs additional comment. With all of the other systems, there is a relatively sharp peak but for VB16 there is only a broad peak. This could indicate an exfoliated structure but may also be indicative of a disordered system.

Table 2. XRD data for PE–clay nanocomposites

| Nanocomposites | 2θ | d-Spacing (nm) | Difference |
|----------------|-----------|----------------|------------|
| PE/6A | 2.42 | 3.6 | 0.2 |
| PE/20A | 2.94 | 3.0 | 0.6 |
| PE/25A | 3.82 | 2.3 | 0.5 |
| PE/MA/VB16 | – | – | – |
| PE/MA/Si18 | 2.48 | 3.5 | 1.3 |
| PE/MA/30B | 2.84 | 3.1 | 1.2 |

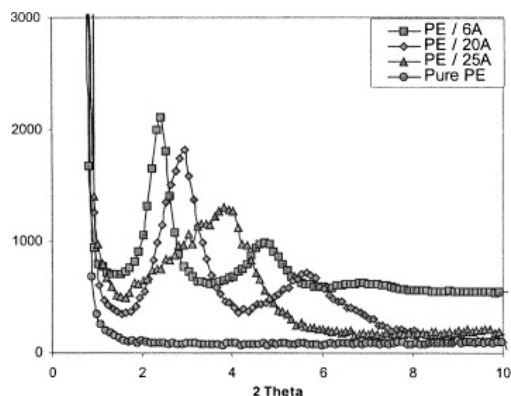


Fig. 1. X-ray diffraction pattern of PE/clay nanocomposites.

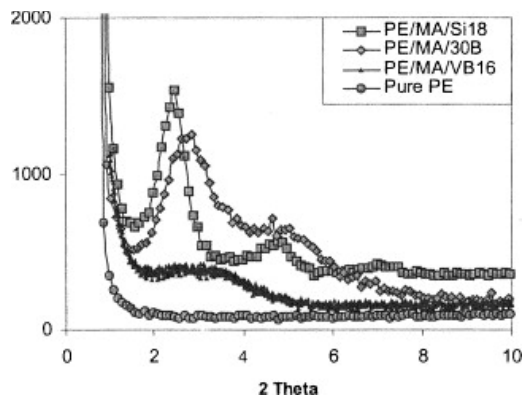


Fig. 2. X-ray diffraction pattern of PE/MA/clay nanocomposites.

It is presumed that there is some reaction that occurs between the MA and the PE which leads to the formation of a graft copolymer in which MA units are attached to the PE chain. No radical initiator was added to the system but, since the reactions were carried out at high temperatures in air, the presence of oxygen can serve the role of initiator and lead to the formation of a graft copolymer. This material may then react with the functionalities on the clay. When the clays that do not have functionalities were used, the presence of MA had no effect on the d-spacing.

3.3. Characterization of nanocomposites by TEM

The results that one obtains from XRD measurements are never sufficient to define the state of the nanocomposite, because of the possibility of disordering of the clay. Thus characterization by TEM is also required. The TEM images of PE/MA/VB16, PE/MA/Si18, PE/MA/30B and PE/25A nanocomposites are shown in Fig. 3, Fig. 4, Fig. 5, Fig. 6. From the low magnification images we can see that the clay is not homogeneously distributed for any of the clays. The clay actually may be well-distributed in some locations but congregated in others. At any rate, one must say that there is some immiscible character to these systems. In the high magnification images one can see that there is clear intercalation for the functionalized clays, while the image for PE/25A, a non-functionalized clay, is much more diffuse and shows a smaller spacing between the clay layers, exactly as seen by XRD. The use of XRD and TEM enables correlation between these techniques and this suggests that the broad peak seen in the PE/MA/VB16 system is actually a peak and is indicative of intercalation. Both Kuchta et al.⁶ and Wang et al.⁷ have reported TEM data for the PE nanocomposites that they have prepared.

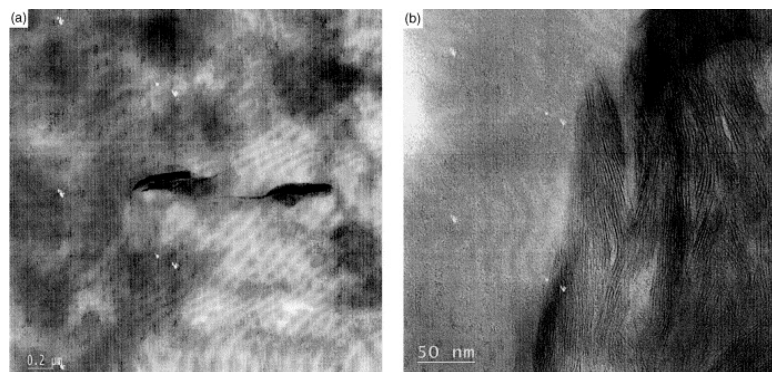


Fig. 3. TEM images of PE/MA/VB16 at (a) low magnification and (b) high magnification.

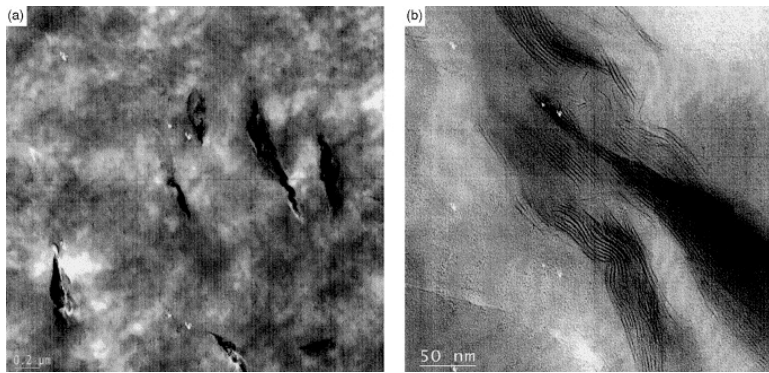


Fig. 4. TEM images of PE/MA/Si18 at (a) low magnification and (b) high magnification.

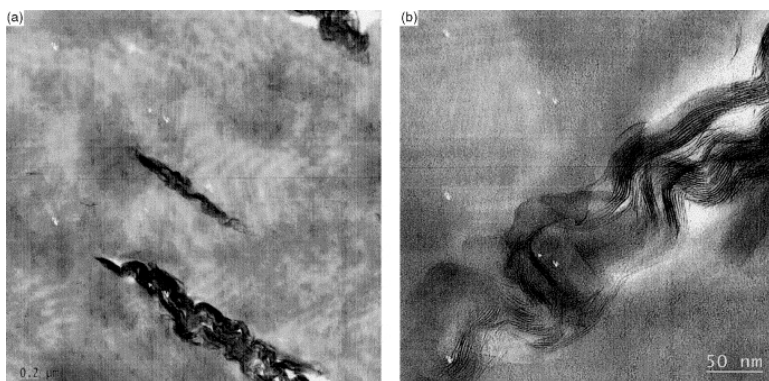


Fig. 5. TEM images of PE/MA/30B at (a) low magnification and (b) high magnification.

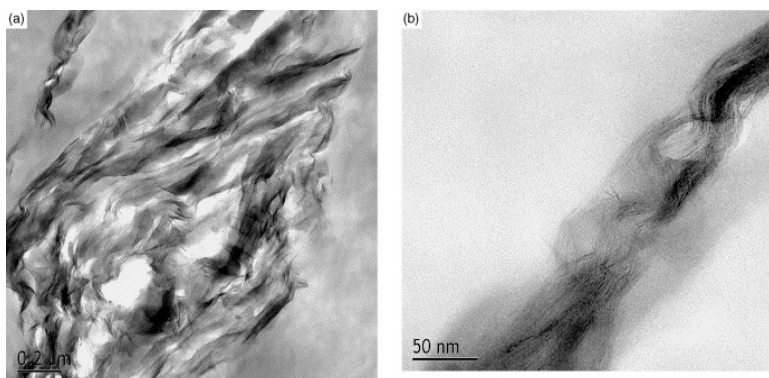


Fig. 6. TEM images of PE/25A at (a) low magnification and (b) high magnification.

3.4. TGA characterization of the nanocomposites

Thermogravimetric analysis provides information on the course of the thermal degradation of the polymer. Table 3 shows the data for the thermal degradation of all of the PE materials. The data which is included is: the temperature at which 10% degradation occurs, $T_{0.1}$, a measure of the onset of the degradation, the temperature at which 50% degradation occurs, $T_{0.5}$, the mid-point of the degradation, and the fraction of material which is non-volatile at 600 °C, denoted as char.¹⁰ This data is also shown graphically in Fig. 7, Fig. 8. There is little change, if any, in the temperature of the degradation and the amount of non-volatile material is simply reflective of the amount of clay that has been added. One must say that nanocomposite formation has almost no effect on the thermal degradation of PE. In previous work it has been observed that for some polymers, notably polystyrene, there is a rather large

change in the onset temperature of thermal degradation while for other polymers, e.g. polyamide-6, there is no change.

Table 3. TGA data, in nitrogen, for PE/clay nanocomposites

| Nanocomposites | $T_{0.1}$ (°C) | $T_{0.5}$ (°C) | Char at 600 °C (%) |
|----------------|----------------|----------------|--------------------|
| Pure PE | 425 | 471 | 1 |
| PE/6A | 432 | 477 | 4 |
| PE/20A | 438 | 478 | 4 |
| PE/25A | 422 | 478 | 4 |
| PE/MA/VB16 | 423 | 475 | 4 |
| PE/MA/Si18 | 435 | 477 | 4 |
| PE/MA/30B | 432 | 478 | 4 |

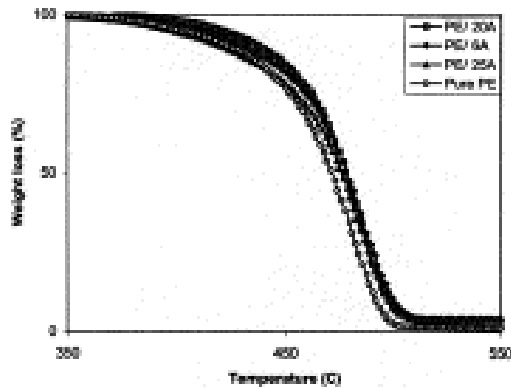


Fig. 7. TGA curves for PE and composites formed using clays which contain no functionalization.

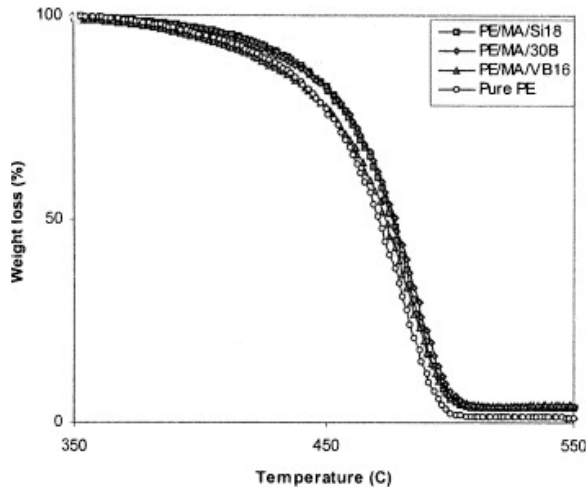


Fig. 8. TGA curves for PE and composites formed using clays which are functionalised.

3.5. Flammability properties of PE–clay nanocomposites

Cone calorimetry provides important information on the fire properties of materials, and it also provides useful information on nanocomposite formation. The parameters which may be measured in the cone calorimeter include, the heat release rate, HRR, the peak heat release rate, PHRR, the specific extinction

area, SEA, a measure of the amount of smoke which is evolved in the combustion, and the mass loss rate, MLR. It has been shown by Gilman that a microcomposite of polyamide-6 shows essentially no reduction in the PHRR while a nanocomposite gives significant reduction in this parameter.⁹ In work carried out in these laboratories, we have observed that microcomposites of polystyrene, poly(methyl methacrylate), and polypropylene do not show a significant reduction in PHRR but all nanocomposites do show this reduction.^{8,11,12} The amount of the reduction is quite variable, depending upon the polymer and ranges between 25% for poly(methyl methacrylate) to 60% for polystyrene or polyamide-6. Thus one characterization of the nanocomposite formation with PE is based upon the reduction in PHRR.

The cone calorimetric results for the various PE nanocomposites are shown in Table 4. The PHRR of all the PE nanocomposites show 30~40% reduction, compared with the pure PE. The heat release rate curves for the pure polymer and its nanocomposites are shown graphically in Fig. 9, Fig. 10. As is typically observed, the total heat released is the same for the nanocomposites as for virgin PE. The SEA is not changed from virgin PE, indicating that the presence of the clay does not cause increased smoke production.

Table 4. Cone calorimeter data for polyethylene and its nanocomposites

| Nanocomposite | $T_{\text{ign}}(\text{s})$ | PHRR [(Kw/m ²)(Δ)%] | Mean SEA (m ² /kg) | Total heat released (MJ/m ²) | Mean MLR [g/(sm) ²] |
|---------------|----------------------------|---------------------------------|-------------------------------|--|---------------------------------|
| Pure PE | 71 | 2100 | 327 | 118 | 30 |
| PE/6A | 95 | 1340 (35) | 416 | 101 | 24 |
| PE/20A | 57 | 1480 (30) | 348 | 111 | 24 |
| PE/25A | 61 | 1500 (30) | 305 | 106 | 26 |
| PE/MA/VB16 | 52 | 1380 (34) | 308 | 110 | 22 |
| PE/MA/30B | 48 | 1450 (31) | 300 | 112 | 24 |
| PE/MA/Si18 | 50 | 1500 (30) | 418 | 112 | 18 |

PHRR: peak heat release rate; SEA: specific extinction area; MLR: mass loss rate.

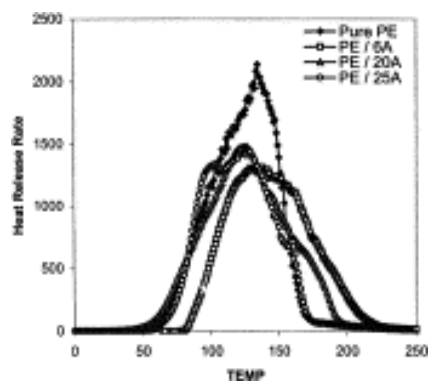


Fig. 9. Comparison of the heat release rate (HRR) plots for pure PE and PE/clay nanocomposites at 35 Kw/m² heat flux.

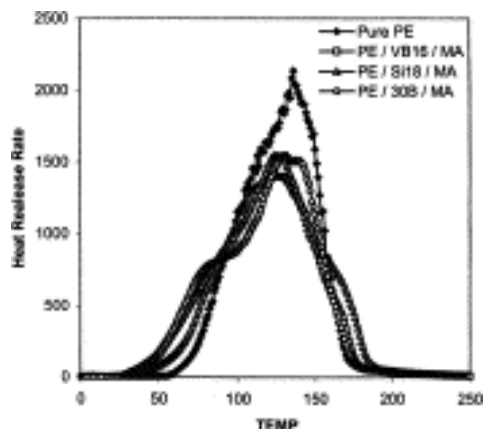


Fig. 10. Comparison of the heat release rate (HRR) plots for pure PE and PE/MA/clay nanocomposites at 35 Kw/m² heat flux.

It is of interest to compare those systems which contain MA with those in which this is absent. The reduction in PHRR and in MLR is about the same whether MA is present or absent. According to the cone criteria presented above for nanocomposite formation, the reduction in PHRR is about the same in all cases so, if nanocomposites are formed in any case, they are formed in all cases.

4. Conclusions

PE–clay nanocomposites have been prepared through melt blending with different organically-modified clays. All of the nanocomposites have a mixed immiscible-intercalated structure. The presence of 3% clay brings about a reduction of 30–40% in the peak heat release rate; this is taken to indicate that nanocomposite formation has occurred in all cases.

Acknowledgements

This work was performed under the sponsorship of the US Department of Commerce, National Institute of Standards and Technology, Grant Number 70NANB6D0119. The assistance of Alexander Morgan and Joseph Harris from the Dow Chemical Company in obtaining the TEM images is gratefully acknowledged.

References

- 1 N. Hasegawa, M. Kawasumi, M. Kato, A. Usuki, A. Okada. *Macromolecules*, 30 (1997), pp. 6333-6338
- 2 J.W. Gilman, C.L. Jackson, A.B. Morgan. *Chem. Mater.*, 12 (2000), pp. 1866-1873
- 3 C. Guo, Z. Liu, D. Xu, D. He, Y. Hu. *Ch J Appl Chem*, 18 (5) (2001), pp. 351-356
- 4 A.M. Dubios. *Polym. Mat.er Sci. Eng.*, 28 (2000), pp. 1-63
- 5 N.G. Gaylord, A. Takahashi. *Polym. Sci. Technol*, 21 (1983), pp. 183-190
- 6 F.-D. Kuchta, P.J. Lemstra, A. Keller, L.F. Batenburg, H.R. Fischer. *Mat.er Res. Soc. Symp. Proc*, 576 (1999), pp. 363-368
- 7 K.H. Wang, M.H. Choi, C.M. Koo, Y.S. Choi, I.J. Chung. *Polymer*, 42 (2001), pp. 9819-9826
- 8 J. Zhu, A.B. Morgan, F.J. Lamellas, C.A. Wilkie. *Chem. Mater.*, 13 (2001), pp. 3774-3780
- 9 Gilman JW, Kashiwagi T, Nyden M, Brown JET, Jackson CL, Lomakin S, Gianellis EP, Manias E. In: Al-Maliaka S, Golovoy A, Wilkie CA, editors. *Chemistry and technology of polymer additives*. London: Blackwell Scientific, 1998. p. 249–265.

- 10 J. Zhu, P. Start, K.A. Mauritz, C.A. Wilkie. *J. Polym. Sci., Part A: Polym. Chem.*, 40 (2002), pp. 1498-1503
- 11 M. Zanetti, G. Camino, D. Canavese, A.B. Morgan, F.J. Lamelas, C.A. Wilkie. *Chem Mater.*, 14 (2002), pp. 189-193
- 12 J. Zhu, P. Start, K.A. Mauritz, C.A. Wilkie. *Polym. Degrad Stab*, 77 (2002), pp. 253-258